SLR Converter Design for Multi-Cell Battery Charging

Alexander L. Julian, Giovanna Oriti, Mark E. Pfender
Electrical and Computer Engineering Dept.
Naval Postgraduate School
Monterey, CA, USA

***Abstract*— Series connected battery cells can use balancing circuits so that each individual cell has the same state of charge (SOC) as the others. In this paper series-loaded resonant (SLR) converters are used to trickle charge individual cells to accomplish this charge equalization goal and increase the reliability of the battery pack. Analytical equations are used to support the design of an SLR converter laboratory prototype. Additionally a physics based model implemented in Matlab/Simulink predicts the hardware behavior. Both analytical solutions and simulations are validated by laboratory experiments.**

I. INTRODUCTION

Series-loaded resonant (SLR) converters [1] are widely used to charge high voltage capacitors [2][3][4]. They have also been used as battery chargers [5][6]. This topology offers several attractive features when operated in discontinuous conduction mode including reduced switching losses and almost constant peak current output independent of the switching frequency when the input voltage and output voltage are constant. This means that the SLR converter behaves like a current source. One of the goals of this paper is to present a set of equations to design SLR converters without using computer simulations. Another goal is to use SLR converters to trickle charge individual battery cells in a multi-cell series configuration to achieve voltage equalization. Lead acid batteries are used in the experimental set up, however the proposed configuration applies to lithium- ion batteries as well.

Many researchers have explored the behavior of an SLR converter. In [7] the efficiency is predicted for varying resistive loads using Orcad PSpice without studying the effect of the circuit impedance. In [2] the resonant current and voltage equations are presented but the efficiency is not studied and the steady state waveforms are not derived. References [3][8] look at the resonant voltage and current analytically but do not identify the steady state solution or study efficiency. This paper presents analysis, design, simulations and experimental validation of an SLR converter used to trickle charge battery cells in a multi-cell configuration.

II. SLR TOPOLOGY AND EQUATIONS

Figure 1 shows the schematic of a series connected battery stack using SLR converters on each cell as charge equalizers. The box labeled "stack charger" represents a converter charging the entire battery stack. Each SLR converter derives its input voltage from the battery stack, while the nominal output is 12V for each battery cell. Because the ground voltage for the input and the output of the SLR converters are different galvanic isolation inside each SLR converter is necessary.

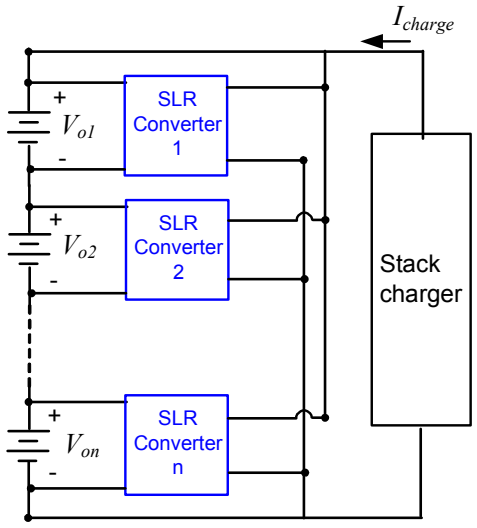

Figure 1. Multicell battery stack set up.

Figure 2 shows the schematic of an SLR converter driving a transformer - diode rectifier - capacitor load. When the half bridge in Figure 2 drives the resonant circuit below ½ of the resonant frequency then discontinuous conduction (DCM) mode occurs. When the circuit is driven above ½ the resonant frequency the continuous conduction mode (CCM) occurs [1].

Several simplifying approximations are made so that a function for the resonant current i_r and the resonant voltage v_r can be derived:

- Diode and IGBT voltage drops are neglected
- The transformer and resonant inductor are ideal and lossless
- The output voltage V_o reflected to the primary is constant

These approximations lead to analytic equations for i_r and v_r which, for $0 < t < t_1$ in Figure 3, are

$$i_r(t) = Ir_0 \cos \omega_o t + \frac{V_s - Vr_0 - V_o}{\omega_o L_r} \sin \omega_o t \qquad (1)$$

$$v_r(t) = (V_s - Vr_0 - V_o)(1 - \cos \omega_o t) + Vr_0 + \frac{Ir_0 \sin \omega_o t}{\omega_o C_r} \qquad (2)$$

where Ir_0 and Vr_0 are the inductor current and capacitor voltage initial conditions, V_s and V_o are the input DC voltage and reflected output DC voltage amplitudes respectively, L_r and C_r are the inductor and capacitor values, and the resonant frequency and circuit impedance are

$$\omega_o = \frac{1}{\sqrt{L_r C_r}}, \quad Z_o = \sqrt{\frac{L_r}{C_r}} \qquad (3)$$

For the time interval $t_1 < t < t_2$:

$$i_r(t) = \frac{V_s - Vr_{t1} + V_o}{\omega_o L_r} \sin \omega_o (t - t_1) \qquad (4)$$

$$v_r(t) = (V_s - Vr_{t1} + V_o)(1 - \cos \omega_o (t - t_1)) + Vr_{t1} \qquad (5)$$

where Ir_{t1} and Vr_{t1} are the inductor current and capacitor voltage initial conditions at $t = t_1$. Note that the sign of the output voltage in (5) is the opposite of the output voltage in (2) because when the current polarity reverses the diode rectifier reverses the voltage on the transformer secondary.

In DCM Ir_0 is zero. As shown in Figure 3, which is a plot of the analytical equations (1) through (5), the current returns to zero at $t = t_1 = \frac{\pi}{\omega_o}$ and again at $t = t_2 = \frac{2\pi}{\omega_o}$. The symmetric operation of the H-bridge with alternating positive and negative voltage pulses means that $Vr_0 = -Vr_{t2}$. The time t_1 is the moment when the current returns to zero so $Ir_{t1}=0$. Evaluating (2) at $t = t_1$ yields

$$Vr_{t1} = Vr_o + 2(V_s - Vr_o - V_o) \qquad (6)$$

Evaluating (5) at $t = t_2 = \frac{2\pi}{\omega_o}$ yields

$$Vr_{t2} = -Vr_{t1} + 2V_s + 2V_o \qquad (7)$$

so $Vr_0 = -2V_o$.

In order to have symmetric operation of the resonant pulses created by each pair of IGBTs in the H-bridge the current in (4) must go negative after $t = t_1$ so the amplitude of (4) is negative. This will discharge the resonant capacitor to the initial value for the next symmetric pulse created by the other pair of IGBTs. Substituting (6) into (4) shows that

$$V_s - Vr_{t1} + V_o = -V_s + V_o < 0 \qquad (8)$$

so $V_s > V_o$ is a necessary constraint for symmetric operation.

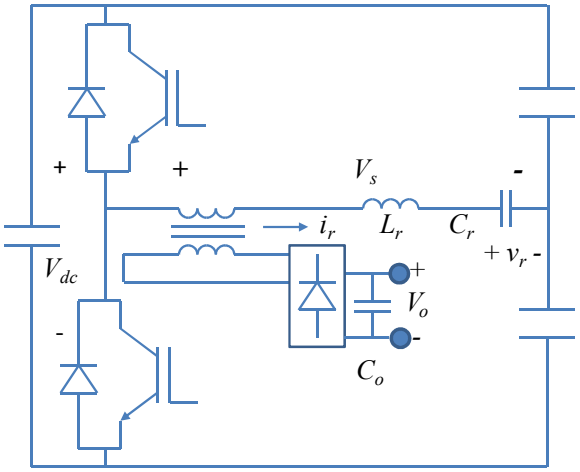

Figure 2. SLR converter circuit schematic.

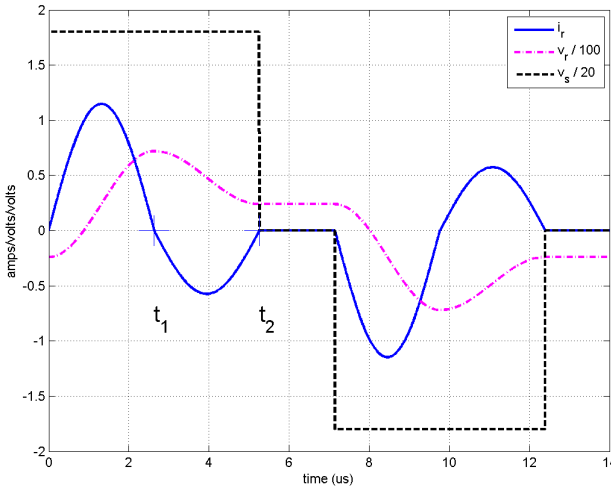

Figure 3. Waveforms from analytical equations for DCM.

III. SLR Converter Analysis in DCM

The ideal analytic equations to represent an SLR converter can provide important insight for the component selection and stress estimation.

A. Circuit design using analytical equations

Equations (1) through (5) are useful to predict the peak current stress and the peak voltage stress for the circuit components including the resonant inductor and capacitor, the transformer, the MOSFETs and the rectifier diodes.

The input voltage is given by six 12V lead acid batteries producing 72V dc output. Since the circuit topology uses a half bridge inverter, $V_s=36V$. The output voltage is nominally 12 V and will vary +/- 1V from the discharged state to the fully charged state. The transformer turns ratio is 1:1.

B. Average DC input current in DCM

Discontinuous conduction mode is achieved when the switching period is

$$T_{sw} \geq \frac{4\pi}{\omega_0} \tag{9}$$

The switching period represents the time for two symmetric pulses to occur. In DCM the input power from the half bridge can be calculated analytically

$$p_{in}(t) = v_s(t) i_r(t) \tag{10}$$

where $i_r(t)$ is defined in (1) for $0<t<t_1$ and (4) for $t_1<t<t_2$. For the symmetric pulse the current must be negated. The average input current from the DC source in DCM is derived using (1) and (4).

$$I_{in\_avg} = \frac{1}{T_{sw}} \int ir(t)\,dt = \frac{2}{T_{sw}} \int_0^{t_1} \frac{V_s + V_o}{\omega_o L_r} \sin \omega_o t\,dt + \frac{2}{T_{sw}} \int_{t_1}^{t_2} \frac{-V_s + V_o}{\omega_o L_r} \sin \omega_o t\,dt = \frac{8V_o}{\omega_o^2 L_r T_{sw}} \tag{11}$$

Equation (11) shows the average input current changes during charging with V_o. When the output voltage varies from 11 to 13 volts and the switching period is 20 μs the average input current changes from 79 *mA* to 94 *mA*.

C. Constant average DC output current in DCM

The average rectified current to the capacitor load in DCM is also derived using (1) and (4):

$$I_{out\_avg} = \frac{1}{T_{sw}} \int |ir(t)|\,dt = \frac{2}{T_{sw}} \int_0^{t_1} \frac{V_s + V_o}{\omega_o L_r} \sin \omega_o t\,dt - \frac{2}{T_{sw}} \int_{t_1}^{t_2} \frac{-V_s + V_o}{\omega_o L_r} \sin \omega_o t\,dt = \frac{8V_s}{\omega_o^2 L_r T_{sw}} \tag{12}$$

Equation (12) shows that the average load current is constant even though the current waveform shape changes whenever the output voltage changes during charging. Since the ideal model is lossless the input power equals the output power.

$$P_{out\_avg} = V_o I_{out\_avg} = \frac{8V_o V_s}{\omega_o^2 L_r T_{sw}} = P_{in\_avg} = V_s I_{in\_avg} \tag{13}$$

The peak current is constant in DCM for a fixed input and output voltage and independent of the switching frequency. When the converter enters CCM the efficiency drops because of the added turn on losses and the peak current increases. Since this application is an unregulated charger the resonant impedance can be chosen to fix the peak current and power flow in DCM while optimizing the efficiency by remaining in DCM. For a fixed peak current the RMS current should be as high as possible to make the best use of the IGBTs. This rationale points to the boundary of CCM and DCM as the best operating point for this application. Continuous operation at the boundary of CCM and DCM will lead to constant output current and increasing output power as the output voltage increases.

D. Constant efficiency in DCM

The efficiency η can be expressed in terms of the power or energy:

$$\eta = \frac{p_{out}}{p_{in}} = \frac{p_{in} - p_{losses}}{p_{in}} = \frac{energy_{in} - energy_{losses}}{energy_{in}} \tag{14}$$

The input energy for one switching period is the integral of the source voltage times the average input current for one switching period:

$$energy_{in} = \int_0^{T_{sw}} V_s I_{in\_avg}\,dt == \frac{8V_s V_o}{\omega_o^2 L_r} \tag{15}$$

In DCM the input energy is constant for each resonant pulse for a fixed input voltage and a fixed output voltage. The energy related to the losses can be considered constant also since the nonzero part of the current waveform doesn't change in DCM. The conduction losses in the semiconductors and the transformer will not change. The switching losses are zero in DCM. Since all of the energy terms in (14) are constant in DCM regardless of the switching frequency the efficiency is constant in DCM.

IV. HARDWARE SET UP

An SLR converter was designed and implemented on a custom printed circuit board (PCB) to trickle charge a 12V battery cell. A photograph is shown in Figure 4.

The SLR converter is controlled by a field programmable gate array (FPGA) based controller and the parameters for the experimental set up are shown in Table I and Table II for two different output voltages, 12.8V and 11.6V respectively. The switching frequency is constant and low enough to ensure DCM. There is no closed loop control on the switching frequency. The duty cycle of the TTL signal driving the MOSFETs is chosen so that the gate signal is removed before the resonant current goes negative during each resonant pulse.

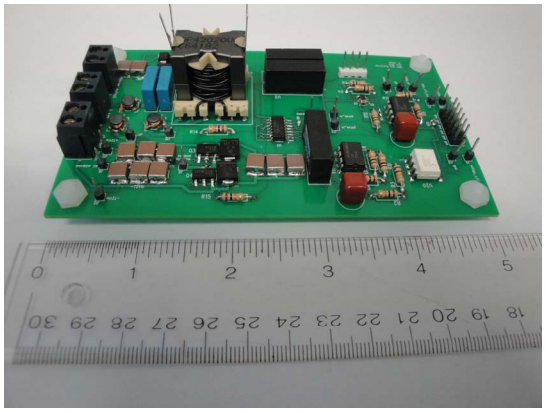

Figure 4. SLR implemented on a custom PCB.

TABLE I. LAB EXPERIMENT PARAMENTERS – 12.8 V OUTPUT

Parameter	Symbol	Value
Resonant capacitors	C_r	*20 nF*
Resonant inductor	L_r	*35 µH*
Output capacitor	C_o	*18.8 µF*
Bus voltage	V_{dc}	*62.4 V*
Magnetizing inductance	L_m	*3.76 mH*
Transformer turns ratio	N_t	*1*
Switching frequency	f_s	*48.6 kHz*
Output voltage	V_o	*12.8 V*
Average output current	I_{out}	*226 mA*

TABLE II. LAB EXPERIMENT PARAMENTERS – 11.6 V OUTPUT

Parameter	Symbol	Value
Resonant capacitors	C_r	*20 nF*
Resonant inductor	L_r	*35 µH*
Output capacitor	C_o	*18.8 µF*
Bus voltage	V_{dc}	*62.4 V*
Magnetizing inductance	L_m	*3.76 mH*
Transformer turns ratio	N_t	*1*
Switching frequency	f_s	*78 kHz*
Output voltage	V_o	*11.6 V*
Average output current	I_{out}	*363 mA*

V. EXPERIMENTAL MEASUREMENTS VS. MODELING

This section compares the experimental measurements with the ideal waveforms and the simulations. The ideal waveforms are created using the analytical equations presented in section III. The simulated waveforms are obtained from a physics based model of the SLR converter implemented in Matlab/Simulink.

Figure 5 compares the simulations to the measured waveforms. The physics based model includes several details to improve the accuracy including:

- IGBT / diode voltage drop
- Transformer hysteresis effect
- Transformer leakage inductance affecting the resonant frequency
- Transformer and inductor winding resistances
- Rectifier diode voltage drops

These features make it possible for the simulated waveforms to closely match the measured data. When the converter is off some high frequency ringing can be observed in the experimental measurements of the resonant current in Figure 5 through Figure 8. This phenomenon is due to the MOSFET capacitance resonating with the resonant inductor. This physical behavior has not been included in the model or the analytical equations.

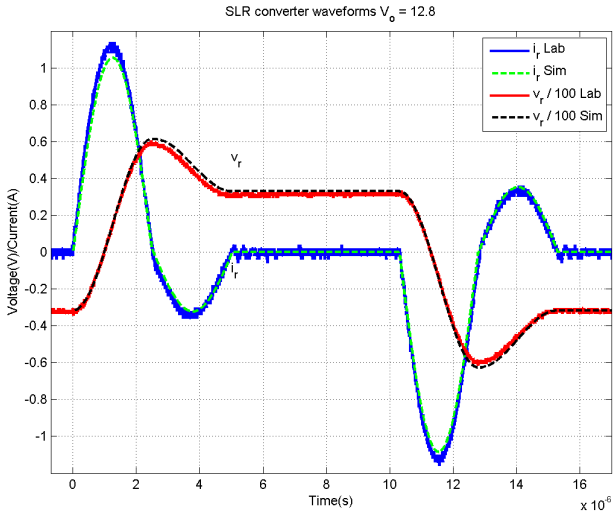

Figure 5. Experimental measurements compared to simulated waveforms with output voltage 12.8V.

In Figure 6 the ideal current, obtained with the analytic equations, is slightly larger because the winding resistances are not considered. However the leakage inductances of the transformer are considered which causes the resonant frequency to match. The output voltage diode drops are also included in the ideal waveforms by adjusting V_o in equations (1), (2), (4), (5) which are used to create the ideal waveforms shown in Figure 6 and Figure 8.

Figure 7 shows the resonant waveforms when the output voltage is lowered to 11.6 volts. Figure 8 shows that the ideal waveforms are good estimates of the measured data when the charging voltage is lower at 11.6 volts.

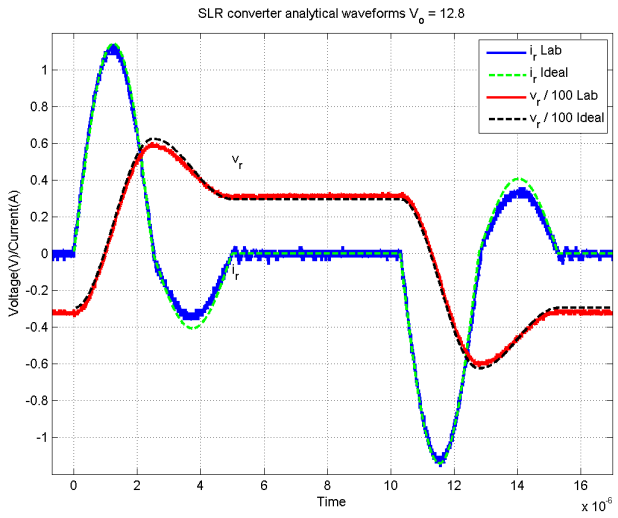

Figure 6. Experimental measurements compared to analytical equations with output voltage 12.8V.

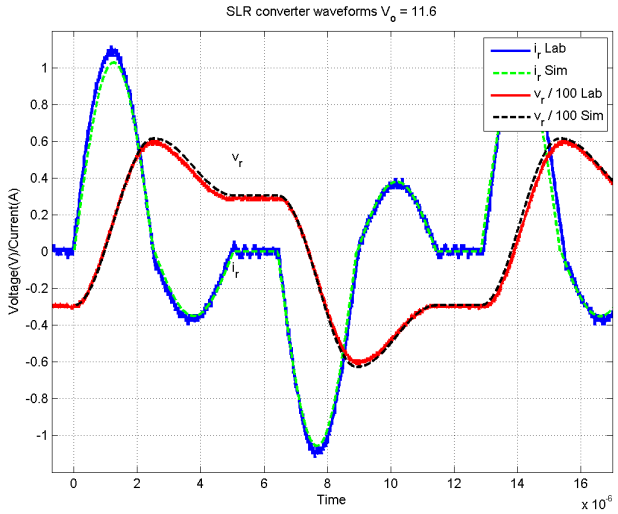

Figure 7. Experimental measurements compared to simulated waveforms with output voltage 11.6V.

Figure 9 shows the SLR converter's DC output voltage when the battery cell voltage is 12.8V. Note that the ripple is at twice the switching frequency because of the diode rectifier.

VI. Conclusions

This paper provides powerful, yet simple tools to assist in the design of SLR converters used to trickle charge individual battery cells in a multi-cell configuration. Using the analytical equations the behavior of the SLR converter is predicted quite accurately. This is confirmed by numerical simulations and experimental measurements. A laboratory prototype was built to charge an individual cell in a battery stack when the voltage is lower or higher than the nominal 12V. Experimental measurements match well with analytical equations and numerical simulations.

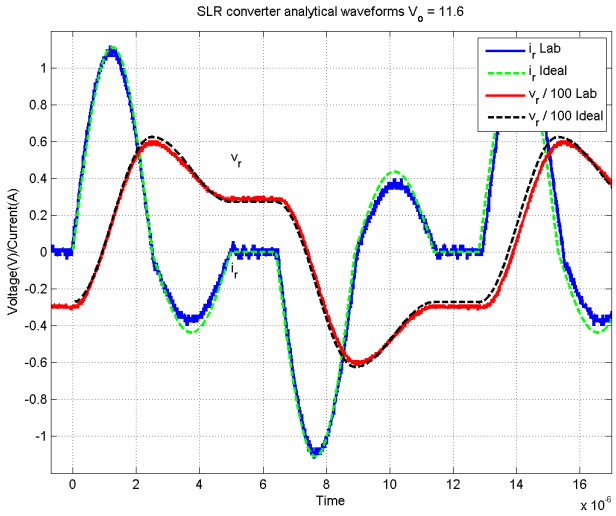

Figure 8. Experimental measurements compared to analytical equations with output voltage 11.6V.

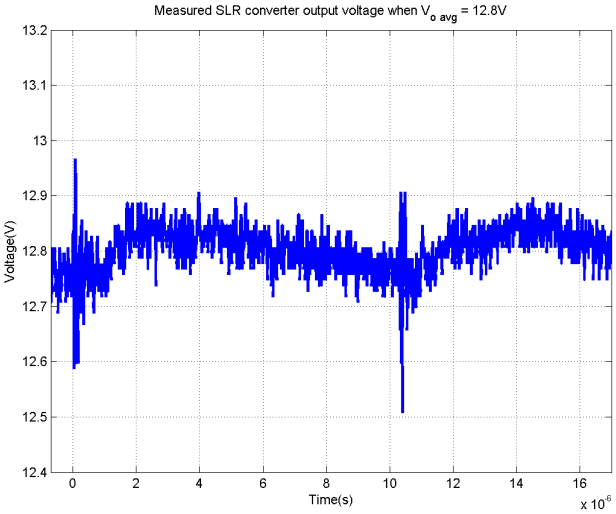

Figure 9. Experimental measurements of the SLR converter output voltage, V_o.

References

[1] N. Mohan, T. Undeland, W.P. Robbins, *Power Electronics*, Converters Applications and Design, third edition, John Wiley and Sons, Inc., 2003.

[2] A. C. Lippincott, R. M. Nelms," A capacitor-charging power supply using a series-resonant topology, constant on-time/variable frequency control and zero-current switching," *IEEE Transactions on Industrial Electronics*, Vol.38, No. 6, 1991, pp.438-447.

[3] D. Feng, J. Sun, J. Long, "Design of High-voltage DC Power Supply Based on Series-Resonant Constant-Current Charging", *in Proc. of 2010 5th IEEE Conference on Industrial Electronics and Applications*, pp 1142-1146.

[4] H. Pollock, "Constant frequency, constant current load-resonant capacitor charging power supply", *Electric Power Applications, IEE Proceedings* - Volume: 146, Issue: 2, 1999, pp 187-192.

[5] Y-C. Chuang, Y-L. Ke, H-S. Chuang, H-K. Chen, "Implementation and analysis of an improved series-loaded resonant DC-DC converter operating above resonance for battery chargers", *IEEE Trans. on Ind. Applications*, Vol.45, no. 3, May/June 2009.

[6] Y-L. Ke; Y-C. Chuang; Y-K. Wu; S-J. Cai, "Photovoltaic energy battery chargers with a series-parallel load resonant converter", *in Proc. of IEEE Industrial and Commercial Power Systems Technical Conference (I&CPS), 2011*.

[7] M. McCarty, T. Taufik, A. Pratama, M. Anwari, "Efficiency performance analysis of series loaded resonant converter", in Proc. of *2009 IEEE Symposium on Industrial Electronics and Applications (ISIEA 2009)*, October 4-6, 2009, Kuala Lumpur, Malaysia.

[8] Y. Zhang, P. E. Bagnoli, "Numerical Analysis of Series-Resonant Charging Converter", *in Proc. of SPEEDAM 2010, International Symposium on Power Electronics, Electrical Drives, Automation and Motion*, pp. 472-477.

[9] G. -H. Rim et al, "A constant current high voltage capacitor charging power supply for pulsed power applications", *Pulsed Power Plasma Science, 2001. IEEE Conference Record, 2001*, pp 1284-1286.